J. Fluid Mech. (1992), *vol.* 243, *pp.* 699–720
Printed in Great Britain

Turbulence measurements in a round jet beneath a free surface

By D. G. ANTHONY[1] AND W. W. WILLMARTH[2]

[1] David Taylor Research Center, Bethesda, MD 20084-5000, USA

[2] Department of Aerospace Engineering, The University of Michigan, Ann Arbor, MI 48109-2140, USA

(Received 19 August 1991 and in revised form 30 April 1992)

The results of an experimental investigation of a turbulent jet flow issuing from a circular nozzle beneath and parallel to a free surface are presented. Measurements of the mean velocity vector and all components of the Reynolds stress tensor were made using a three-component, underwater laser-Doppler velocimeter (LDV). Visualizations of the flow field using both fluorescent dye and free-surface shadowgraphs were made in support of the measurements. The jet is observed to form a shallow surface current, the lateral extent of which is significantly greater than that of the primary jet flow that produces it. Flow visualization reveals the surface current to consist largely of fluid structures ejected from the jet. These structures remain coherent within the current, apparently as a consequence of reduced turbulent mixing just beneath the surface. LDV measurements of the turbulence within the surface current reveal that near the jet centreline, where the interaction between the jet and the free surface is most intense, the velocity fluctuations normal to the free surface are diminished in approaching the surface, while the fluctuations parallel to the surface are enhanced. Away from the jet centreline, toward the edges of the surface current, the vertical and cross-stream fluctuations become approximately equal in magnitude, whereas the streamwise fluctuations become diminished. This is attributed, in part, to orbital motions beneath surface waves generated by the interaction of large-scale jet structures with the surface. When oleyl alcohol, an insoluble surface-active agent, was added to the free surface, the surface current was not observed. Comparisons between a jet issuing beneath both clean and surfactant-contaminated free surfaces,and a jet issuing beneath a solid wall are made to identify the role of streamwise vorticity and of secondary vorticity generated at boundaries on the development of these flows.

1. Introduction

The behaviour of turbulent flows adjacent to a free surface is of considerable interest to the remote detection of the wakes of surface ships. Synthetic Aperture Radar images of the ocean surface reveal distinctive signatures characteristic of the ship's turbulent wake and persisting for many kilometres behind the vessel. These signatures have been attributed to surface disturbances created by the hull and propulsion system (Lyden *et al.* 1988) and to short-wavelength surface waves generated behind the ship (Munk, Scully-Power & Zachariesen 1987).

The present investigation of the flow field and behaviour of a turbulent jet issuing beneath a free surface is intended to provide some understanding of the hydrodynamic mechanisms that govern the interactions among turbulence, surface

waves, and surface currents in the wake of a ship. The relevance of this flow to the flow in a ship's wake arises from consideration of the momentum balance within the turbulent wake of a self-propelled ship. The ship's propulsion system must overcome not only the viscous resistance of the hull, but also its wavemaking resistance, of approximately the same magnitude. Because the wave system propagates away from the centreline region, the turbulent wake of a self-propelled ship contains an excess of momentum, and thus resembles a submerged, turbulent jet.

There is considerable literature devoted to the characteristics of axisymmetric turbulent free jets; Abramovich (1963) and Rajaratnam (1976) offer comprehensive reviews. Extensive turbulence measurements in the self-similar or self-preserving region of the axisymmetric jet have been reported by Wygnanski & Fiedler (1969) in a particularly thorough investigation.

Investigations of turbulent jet flows near free surfaces have, until recently, been concerned primarily with flows of relevance to civil and hydraulic engineering, where the effects of buoyancy are often significant. Rajaratnam & Humphries (1984) investigated the scaling behaviour of the mean flow field of turbulent, non-buoyant surface jets, and Rajaratnam & Subramanyan (1985) investigated that of planar buoyant surface jets. Swean *et al.* (1989) report measurements of mean velocities and turbulent fluctuations in a two-dimensional turbulent jet issuing at a free surface. They conclude that the growth rates of the length and velocity scales resemble those of a two-dimensional wall jet at the same Reynolds number.

An experimental investigation of the interaction of a round turbulent jet with a free surface was reported by Bernal & Madnia (1988). Mean flow and turbulence measurements of the streamwise velocity component were made using a hot-film anemometer, and an image model was shown to describe the scaling of the mean flow field. The free surface was regarded as a symmetry plane, for low Froude numbers, and three self-similar regions were identified, depending on the relative magnitudes of downstream distance x and depth h. If the jet is sufficiently far from the free surface, there is a self-similar region in which the jet behaves like the free jet ($x \ll h$). Far downstream, the jet again behaves like the free jet, but with twice the momentum to account for the effect of the image jet ($x \gg h$). Between these two regions, there is an interaction region in which the jet depth h is the dominant lengthscale, and within this region, a family of self-similar mean velocity profiles scaling with x/h is obtained. The mean streamwise velocity profiles have their maxima occurring above the jet centreline, and in this respect resemble those of the wall jet.

An investigation by Liepmann (1990) showed that instabilities in the near-field region of a round jet are strongly influenced by the presence of a free surface, and that the jet flow field is altered through changes in the entrainment field near the free surface.

The free-surface jet can be compared to a wall jet having the same geometry, but differing in the surface boundary condition. Newman *et al.* (1972) studied a three-dimensional wall jet with the jet orifice affixed to the wall ($h/d \approx 0.5$, where d is jet diameter) and reported that the rate of growth of the lengthscale parallel to the wall was significantly greater than that normal to the wall. Davis & Winarto (1980) showed that wall jets, at depths ranging from $h/d = 0.5$ to 4, become increasingly oblate with downstream distance, the growth rate of the lengthscale parallel to the wall becoming many times larger than that normal to the wall at large distances from the nozzle. Their measurements show that turbulent mixing parallel to the wall exceeds that normal to the wall, and that the interaction between the jet and wall

involves coherent motion with inflow normal to the wall and outflow parallel to the wall. Launder & Rodi (1981, 1983) further document the disparity in lateral and normal spreading rates among wall jets, and show the lateral spreading angle to be highly sensitive to Reynolds number. They attribute differences in the behaviour among various wall jets at the same Reynolds number to differing jet geometries at the discharge plane. The authors postulate that the mechanism acting to produce the observed spreading phenomena is the creation of substantial streamwise vorticity, either from bending of vortex lines or through inhomogeneities in the Reynolds stress field. Unfortunately, the lack of experimental data for the Reynolds stress field makes it difficult to assess the relative importance of these two possible mechanisms (Launder & Rodi 1981).

Measurements of turbulence beneath a free surface have been reported for two-dimensional flows in open channels. Komori *et al.* (1982) measured the turbulent fluctuations and Reynolds stress beneath a free surface in an open channel flow using a laser velocimeter. Their measurements show that the velocity fluctuations become anisotropic as the free surface is approached, those normal to the surface becoming diminished while those parallel to the surface are enhanced. Rashidi & Banerjee (1988) used data obtained from flow visualizations of bubble streaks to reach the same conclusion: near a free surface, the turbulent energy is redistributed from the normal to the parallel fluctuations. The hot-film measurements of Swean *et al.* (1989) for the two-dimensional surface jet also show the turbulent fluctuations to become anisotropic in this manner as the free surface is approached.

In the present investigation, the flow field of a round turbulent jet discharging beneath and parallel to a free surface is studied experimentally. Three-component LDV measurements of the mean flow field and turbulence quantities, including all components of the Reynolds stress tensor, and flow visualizations using laser-induced fluorescence are presented for a shallow jet at a Reynolds number $U_e d/\nu$ of 12700, a Froude number $U_e/(gh)^{\frac{1}{2}}$ of 5.66, and depth h of two diameters. These values were within the range studied by Bernal & Madnia (1988). Particular care was taken to clean the free surface of surface-active agents. It has been observed that surfactants have a strong influence on the trajectories of vortex rings and pairs propagating toward a free surface (Bernal *et al.* 1989; Hirsa 1990) This suggests that surfactants may have an important effect on vortical structures in turbulent flows at a free surface.

Under the conditions investigated, the jet interaction with the free surface is highly three-dimensional, giving rise to considerable surface deformations and to the generation of surface waves. The measurements reveal similarities between the free-surface jet and three-dimensional wall jets, and surfactants are found to change the lateral spreading rate of the jet.

2. Experimental equipment and procedure

2.1. *The laser-Doppler velocimeter*

Three components of velocity were measured simultaneously using a laser-Doppler velocimeter (LDV) designed for velocity measurements in a towing tank (Willmarth 1987). In this design, both the last optical component that transmits light to the measuring volume and the first optical component that receives scattered light from the measuring volume were completely underwater. The LDV was a three-colour, six-beam system that measured three non-orthogonal velocity components simultaneously; the green (514.5 nm) and blue (488.0 nm) beam pairs determined two

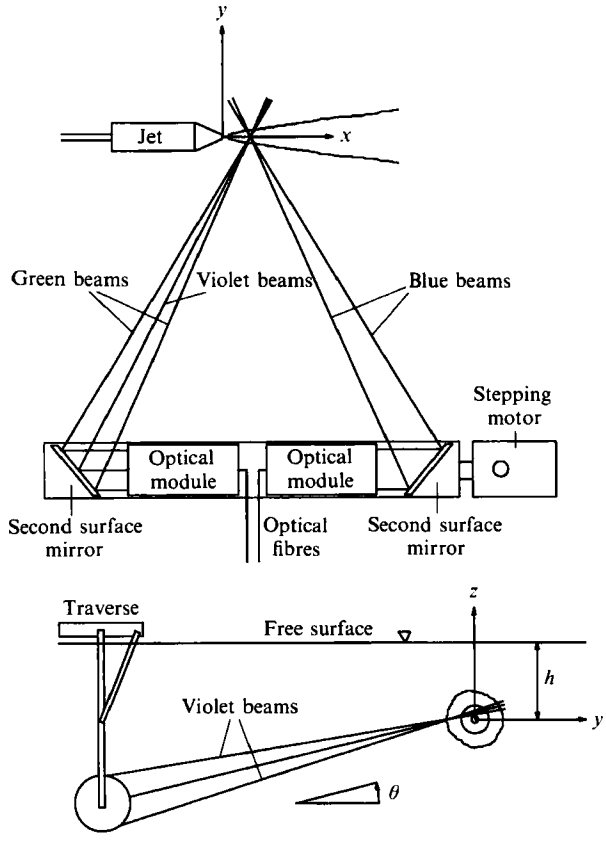

FIGURE 1. Plan and side views of the LDV probe and jet nozzle. The LDV rotates about its axis and translates perpendicular to the jet; the jet translates along its axis.

velocity components in a plane, and the violet (476.5 nm) beams determined the third component, perpendicular to this plane. One of each beam pair was frequency shifted using a Bragg cell modulated at 40 MHz in order to distinguish reversed flow on any component. Optical fibres were used to transmit light between the underwater and the above-water optics.

The underwater optics were contained in two modules mounted oppositely in a cylindrical housing, and a pair of underwater, second-surface mirrors folded the six beams to a crossing at approximately 1.25 m from the housing axis. The three beam pairs of the LDV formed ellipsoidal measurement volumes each approximately 0.020 cm in diameter and 0.47 cm in length. The measurement volumes from the two modules overlapped, and the angle between their optical axes was approximately 53°. As a result, the effective measurement volume length was approximately 0.050 cm. The scattered light was collected off-axis, each of the two modules receiving the light transmitted to the measurement volume by the opposite module; this arrangement led to improved signal-to-noise ratio over the alternative direct backscatter arrangement. The LDV configuration is shown in figure 1.

The three photodetector signals were downmixed against reference frequencies derived from those used to drive their corresponding Bragg cells, and the resulting signals were filtered using Krohn-Hite bandpass filters. The filtered signals were input to three TSI 1980B LDV counter signal processors. The digital outputs of the three signal processors were passed to a data interface which allowed a simultaneity

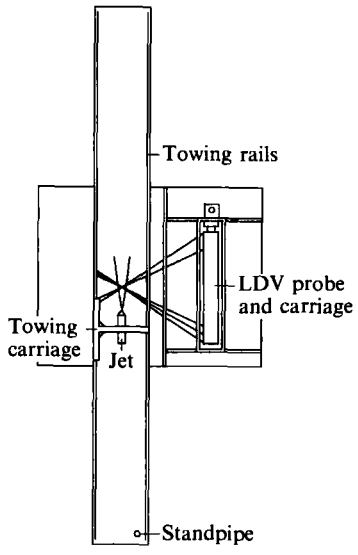

FIGURE 2. Schematic of the towing tank, LDV probe, and jet nozzle.

criterion to be placed on the data: all three processors must have reported valid Doppler information within a specified time window, or the data were discarded. The time window was set equal to the average transit time of scattering particles passing through the LDV measurement volume and typically varied from 0.1 to 10 ms across the flow. A one MHz clock within the interface additionally provided the time between data points. The data were transferred to a LeCroy MM8206A CAMAC digital memory and was then transferred over an IEEE-488 (GPIB) interface to an IBM PC-AT computer.

The LDV was suspended from a carriage that allowed translation parallel to the free surface in a direction perpendicular to the axis of the LDV housing. A stepping motor and gear reducer (harmonic drive) housed in a watertight container attached to the LDV allowed the LDV to be rotated about its axis. This allowed the measurement volume to be positioned just beneath the free surface, through a combination of translation and rotation, without any of the beams being interrupted by the surface. The LDV was designed by one of the authors (Willmarth 1987) in collaboration with TSI, Inc. and was manufactured by TSI, Inc.

The data reported are ensemble averages of many simultaneous, three-component velocity realizations; typically, at least 1000 individual measurements were made at each location. Velocity histograms and statistics were continually updated as the data were obtained, and this information was used to determine the number of data points required for acceptably converged averages. Simultaneous data rates typically varied between about 5 and 30 Hz. Because of the low data rates, time-resolved measurements of the turbulent fluctuations were not possible. The mean and fluctuating velocity data were corrected for velocity bias by weighting each individual velocity measurement with the reciprocal of its magnitude (McLaughlin & Tiederman 1973).

2.2. *The towing-tank facility*

The measurements were made in a 2400-gallon glass-walled towing tank at the University of Michigan. The towing tank and LDV are shown in figure 2, and the towing tank facility has been described in detail by Hirsa (1990). The underwater jet nozzle was suspended from the tank's towing carriage. The water in the towing tank

was continuously filtered through a canister filter to which diatomaceous earth had been added; this was done both to removed suspended rust and dirt, down to about 1 μm in size, and to maintain a uniform temperature throughout the facility. Titanium dioxide particles of the rutile crystalline form were added to the tank prior to measurement as light-scattering seed for the LDV; these particles were approximately 3 μm in size. The filter was not operated when taking measurements, in order to avoid removing seeding particles and to limit recirculation within the towing tank to that caused by the jet itself. A standpipe in the towing tank allowed the free surface to be mechanically cleaned of surfactants prior to taking measurements.

2.3. *The jet nozzle*

The jet consisted of a brass nozzle attached to a settling chamber constructed of concentric lengths of PVC pipe. The inner pipe was cut into sections, serving as spacers between the inlet, honeycomb, screens, and nozzle. The nozzle inlet diameter was 5.90 cm and the exit diameter was 0.635 cm, giving an area contraction ratio of 86:1. The nozzle profile was a fifth-degree polynomial having specified diameter at inlet and exit and both zero slope and curvature at inlet and exit. The jet was supplied from a reservoir tank under the action of gravity, and the reservoir was maintained at constant head by a pump and standpipe. Seeding uniformity between water issuing from the jet and the ambient water was maintained by having the pump draw from, and the jet and reservoir standpipe discharge into, the towing tank facility. The jet was suspended from the towing carriage, and translation of the carriage provided the third axis of positioning. The jet was free to entrain fluid from all direction, in contrast to those emanating from solid walls, e.g. Bernal & Madnia (1988).

2.4. *Flow visualization*

Flow visualization utilizing a laser-induced fluorescence (LIF) technique was used to reveal information about the structure of the surface current. The jet reservoir was filled with a 3 p.p.m. solution of fluorescein dye, and a laser light sheet, formed by passing the blue (488.0 mm) line of an argon-ion laser through a plano-cylindrical lens, was used to excite the dye. The light sheet was oriented either parallel to or normal to the free surface. Still photographs of the illuminated dye were taken through the glass bottom and walls of the towing tank with a Nikon FM-2 camera and 135 mm f2.8 Nikkor telephoto lens using Kodak T-Max 400 film.

Free-surface deformations were visualized using a shadowgraph technique. Collimated light from a mercury arclamp source was transmitted upward through the glass bottom of the towing tank so that it passed through the free surface from below. A piece of ground glass above the free surface was used as an imaging screen, and the shadowgraph images were recorded on video tape so that estimates of the surface wave properties could be obtained. A field of view of approximately 30 cm square was obtained.

2.5. *Surfactants*

The towing tank facility was equipped with a standpipe for mechanically removing surfactants from the free surface. The surface film was drawn off through the standpipe as water was added to the tank, and a fan at the opposite end of the tank was used to generate a gentle surface motion towards the standpipe. Oleyl alcohol, an insoluble surfactant for which the state relationship between surface pressure or surface tension and surfactant concentration is well established (Gaines 1966; Hirsa 1990), was used to contaminate an otherwise clean free surface. A quantity of oleyl alcohol was dissolved in benzene, and the solution was added to the facility surface

x/d	U_e/U_c	U_m/U_c
4	1.00	1.00
8	1.25	1.00
12	1.70	1.00
16	2.24	1.00
20	2.73	1.00
24	3.41	1.00
28	3.96	1.00
32	4.59	1.05
48	6.58	1.13
64	8.41	1.27

TABLE 1. LDV measurements of the centreline ($y = 0$, $z = 0$) and maximum ($y = 0$, $0 \leqslant z/d = \leqslant 2$) mean velocity for the shallow jet, $Re \approx 12700$, $Fr \approx 5.66$, $h/d = 2$

with a pipette, giving the desired reduction in surface tension once the benzene had evaporated. There is at present no established way to measure the spatially and temporally varying surfactant concentration or surface tension dynamically. Only the initial average surface tension, inferred from the initial concentration and the state relationship, is reported.

3. Experimental results and discussion

3.1. *LDV measurements*

Simultaneous three-component velocity measurements were made both for a free jet ($h/d = 50$) and for a shallow jet ($h/d = 2$) to investigate the effects of the free surface on the development of the jet, both in its mean flow and turbulence characteristics. The jet diameter d and exit velocity U_e were 0.635 cm and 200 cm/s, respectively, giving a Reynolds number $Re \equiv U_e d/\nu \approx 12700$ and a Froude number,

$$Fr \equiv U_e/(gh)^{\frac{1}{2}} \approx 5.66$$

for the shallow case.

For the measurements reported, the origin of the coordinate system is on the jet centreline at the jet exit. The streamwise coordinate is x, positive downstream, and the vertical coordinate is z, positive toward the free surface. The cross-stream coordinate is y, defined to make xyz right-handed (figure 1). Measurements were made primarily at downstream distances of $x/d = 16$, 24, and 32; limited measurements were made also at $x/d = 48$ and 64.

The free-jet measurements agree well with those reported by Wygnanski & Fiedler (1969) for the mean flow, but the measured turbulence intensities are some 10% below those of the self-preserving jet and increase with increasing distance downstream. This is to be expected, as Wygnanski & Fiedler have shown that although the mean flow appears self-similar in a few as 20 diameters downstream, it is not until beyond about 70 diameters that the turbulence quantities have achieved a self-preserving character. The measurements reported here correspond therefore to a developing jet beneath a free surface. The free-jet measurements are omitted here for brevity, but are given in Anthony (1990).

Velocity measurements in the flow field of the shallow jet, with $h/d = 2$, were made initially along the jet centreline ($y = 0$, $z = 0$) and later in vertical profiles in the jet centreplane ($y = 0$). The mean velocity U_c, measured along the jet centreline, and the maximum mean velocity U_m, occurring above the centreline but below

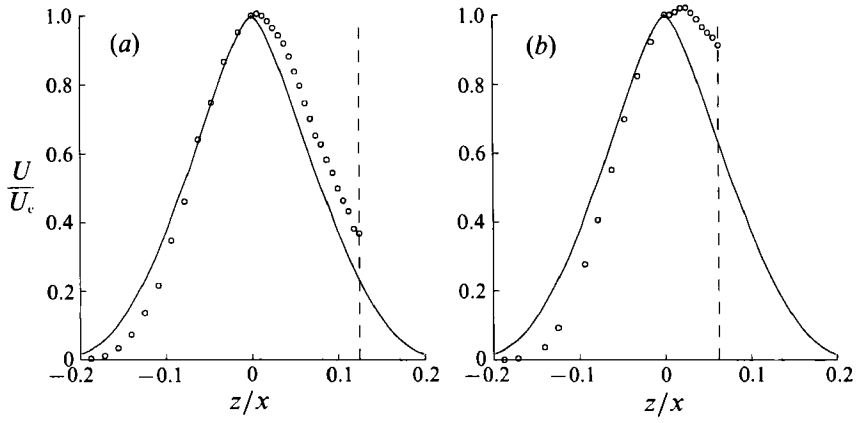

FIGURE 3. Vertical profile of the streamwise mean velocity at (*a*) $x/d = 16$ and (*b*) $x/d = 32$ for the shallow jet, $h/d = 2$, $y/d = 0$. The vertical dashed line at $z/x = 0.125$ in (*a*) and $z/x = 0.0625$ in (*b*) indicates the position of the undisturbed free surface, and the solid curve is the free-jet solution of Tollmien.

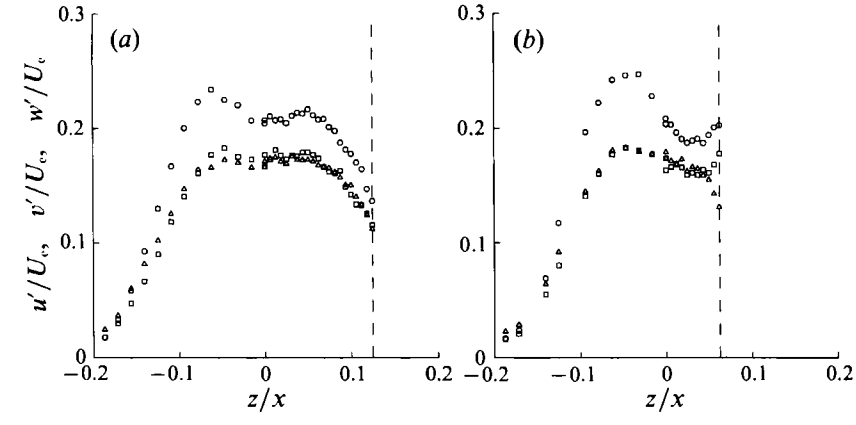

FIGURE 4. Vertical profiles of the RMS velocity fluctuations at (*a*) $x/d = 16$ and (*b*) $x/d = 32$ for the shallow jet, $h/d = 2$, $y/d = 0$. ○, u'; □, v'; △, w'. The dashed line denotes the free surface.

the free surface beyond $x/d = 32$, are tabulated in table 1. The jet exit velocity was $U_e = 200$ cm/s.

Vertical profiles of the mean streamwise velocity at $x/d = 16$ and 32 are shown in figures 3(*a*) and 3(*b*), plotted in the similarity variables of the free jet. The profiles are compared with the free-jet solution of Tollmien, indicated by the solid curve, and the effect of the free surface is to shift the profile toward the surface. The maximum velocity across the profile is no longer at the jet centreline, but moves toward the free surface with increasing distance downstream. This is characteristic of the velocity profiles reported for the surface jet of Bernal & Madnia (1988) within the interaction region.

Figures 4(*a*) and 4(*b*) show a comparison of the turbulent fluctuations at $x/d = 16$ and 32, in vertical profiles through the jet centreline. The data at $x/d = 16$ do not show a significant effect of the free surface, but those at $x/d = 32$ demonstrate a distinctive behaviour very near the surface. Beneath the free surface at $x/d = 32$ (figure 4*b*), the kinetic energy of the turbulent fluctuations is redistributed from the fluctuations normal to the surface to those parallel to it. The magnitude of the vertical fluctuations is diminished, while the magnitudes of the streamwise and cross-

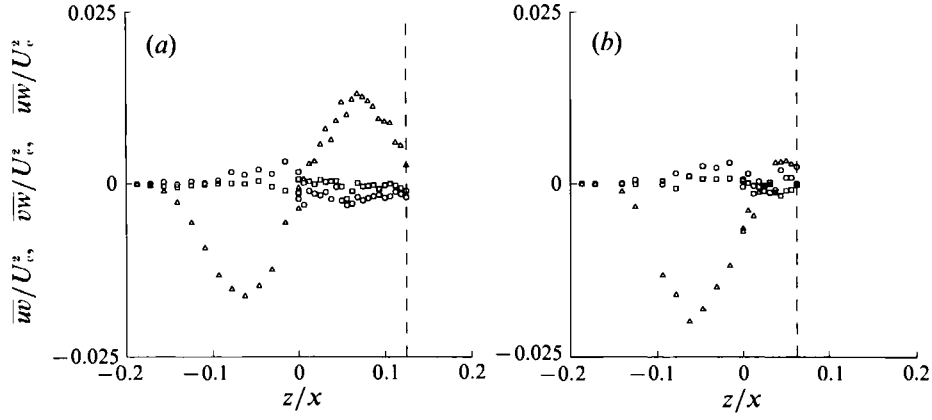

FIGURE 5. Vertical profiles of the Reynolds stresses at (*a*) $x/d = 16$ and (*b*) $x/d = 32$ for the shallow jet, $h/d = 2$, $y/d = 0$. ○, $\overline{uv}$; □, $\overline{vw}$; △, $\overline{uw}$. The dashed line denotes the free surface.

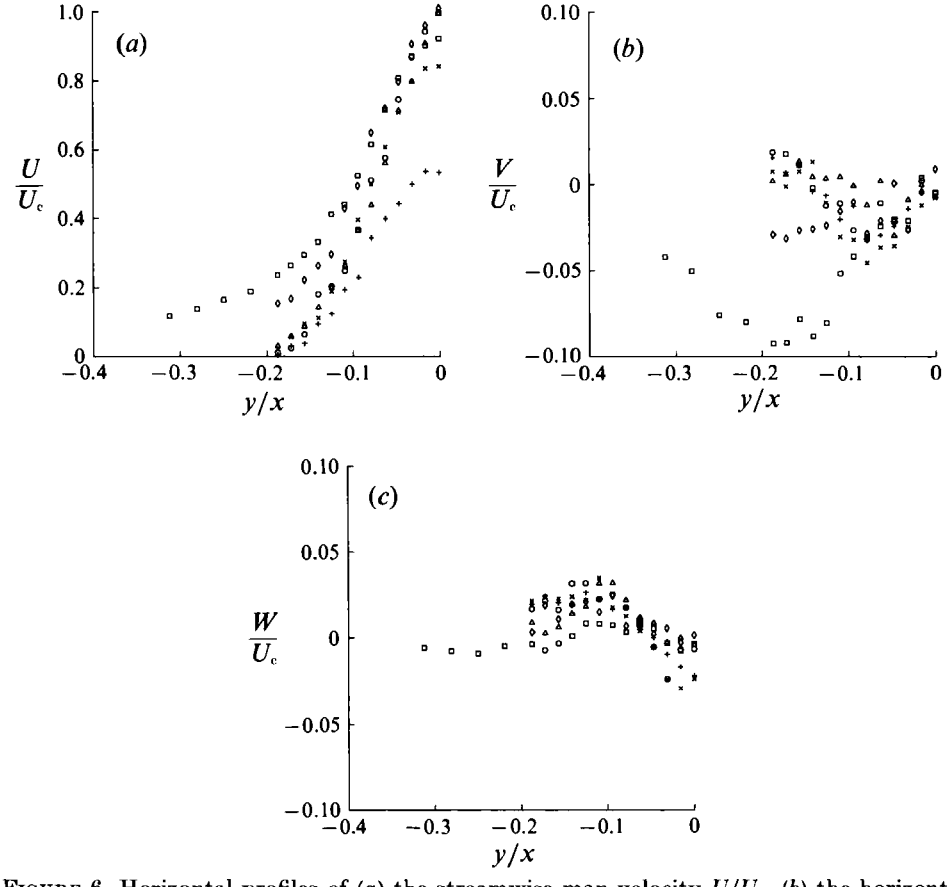

FIGURE 6. Horizontal profiles of (*a*) the streamwise man velocity U/U_c, (*b*) the horizontal mean velocity V/U_c and (*c*) the vertical mean velocity W/U_c, at $x/d = 32$ for the shallow jet, $h/d = 2$. □, $z/d = 2$; ◇, $z/d = 1.5$; △, $z/d = 1$; ○, $z/d = 0$; ×, $z/d = -1$; +, $z/d = -2$.

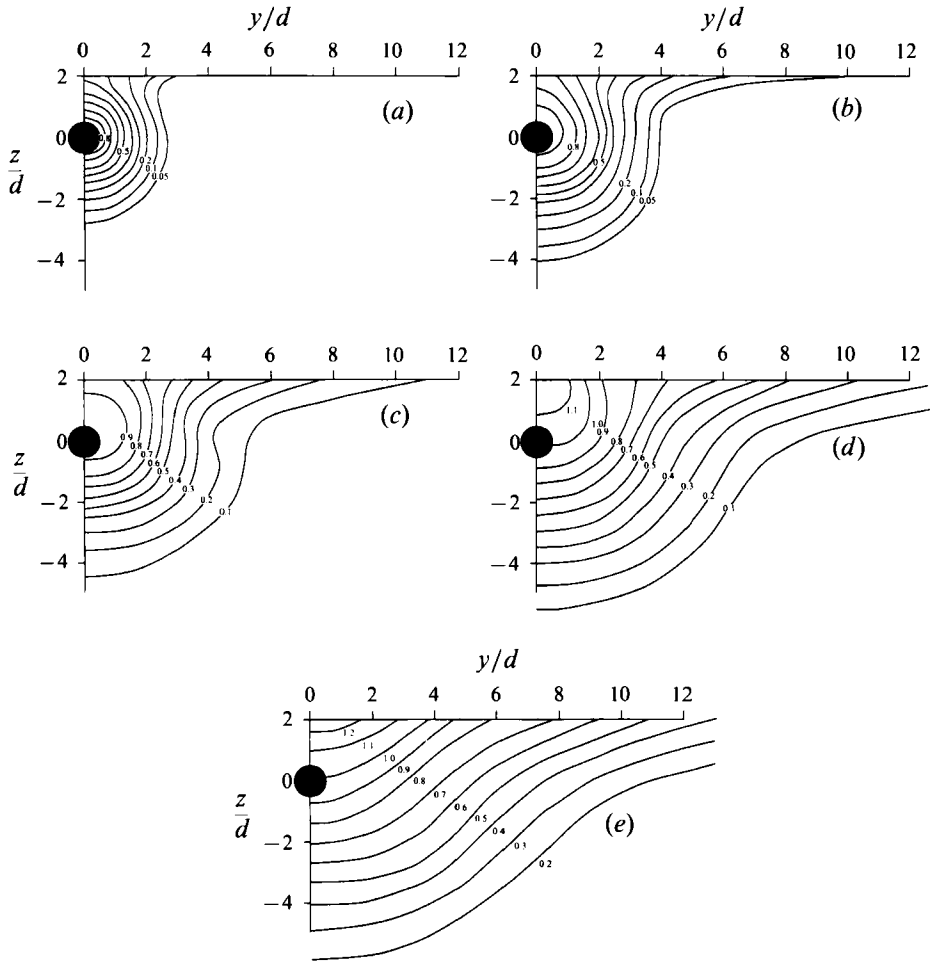

FIGURE 7. Contours of the streamwise mean velocity U/U_c for the shallow jet, $h/d = 2$: (*a*) $x/d = 16$, (*b*) $x/d = 24$, (*c*) $x/d = 32$, (*d*) $x/d = 48$, (*e*) $x/d = 64$.

stream fluctuations are enhanced. Measurements of turbulence beneath free surfaces in two-dimensional turbulent flows have shown similar results (e.g. Komori *et al.* 1982; Rashidi & Banerjee 1988; Swean *et al.* 1989). It was suggested by Anthony, Hirsa & Willmarth (1991) that the alignment of vortex filaments normal to a free surface may be relevant as a mechanism for the observed redistribution of turbulent kinetic energy at a free surface.

The Reynolds stress profiles at $x/d = 16$ and 32, at $y/d = 0$, are compared in figures 5(*a*) and 5(*b*). The stress $\overline{uw}$ tends to zero as the free surface is approached; $\overline{uv}$ and $\overline{vw}$ are nearly zero as required by symmetry. Comparison with figures 3(*a*) and 3(*b*) reveals that the energy production term $-\overline{uw}(\partial U/\partial z)$ is positive throughout these profiles; the transfer of energy is from the mean flow to the turbulence.

Measurements were made along horizontal lines at varying distances above and below the jet centreline, at $x/d = 16$, 24, and 32. The data at $x/d = 32$ are presented here; those at $x/d = 16$ and 24 are reported in Anthony (1990). The streamwise mean velocity profiles at $x/d = 32$, shown in figure 6(*a*), reveal that the jet becomes much wider as the free surface is approached and that this widening is confined to a very shallow layer near the surface. The profile at $z/d = 1$ is little different from that on

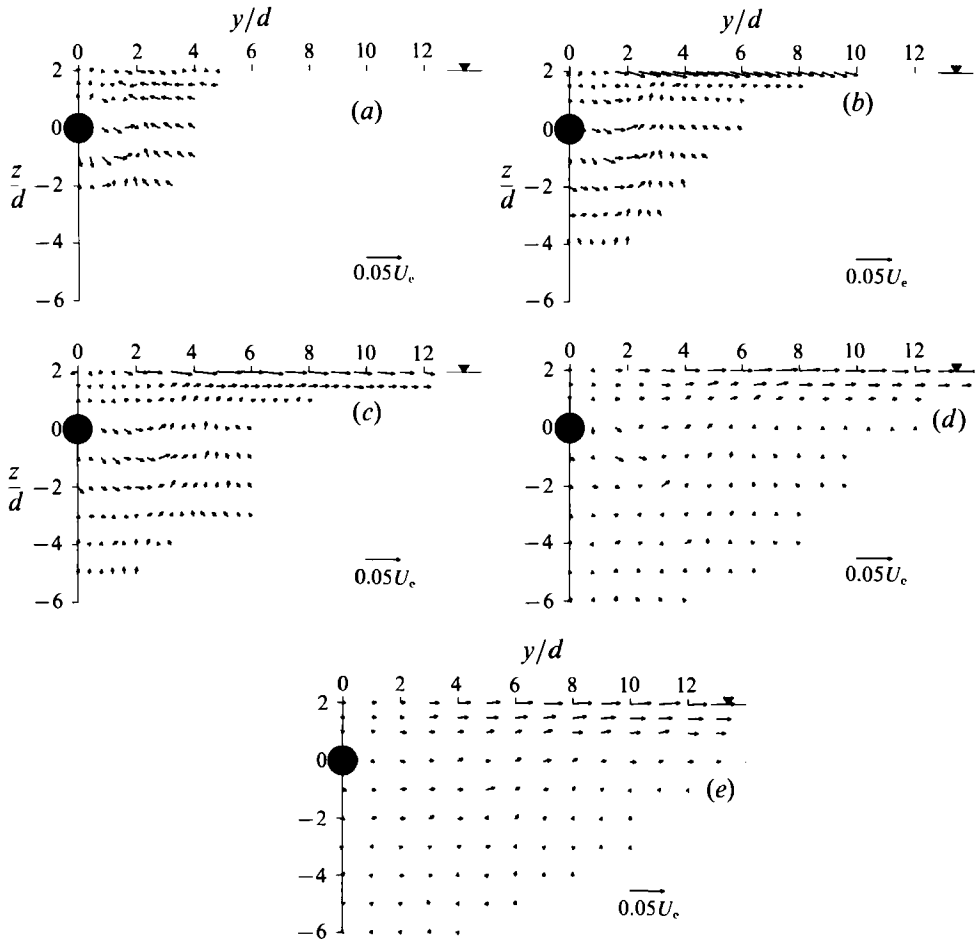

FIGURE 8. Vector plot of the horizontal and vertical mean velocities for the shallow jet, $h/d = 2$: (*a*) $x/d = 16$, (*b*) $x/d = 24$, (*c*) $x/d = 32$, (*d*) $x/d = 48$, (*e*) $x/d = 64$.

the jet centreline $z/d = 0$, yet the tails of the profile at $z/d = 2$ extend to beyond twice the width of those at $z/d = 0$.

Figure 6(*b*) shows the horizontal mean velocity profiles, positive values corresponding to entrainment inward from the sides and negative values to outward growth of the shear layer. The data obtained just beneath the free surface show the mean flow to be everywhere outward, away from the jet centreline, rather than entraining at the edges. The vertical mean velocity profiles, figure 6(*c*), show that there is negligible vertical mean velocity near the surface.

In summary, the mean flow data at $x/d = 32$ show that beneath a free surface that is essentially free of surfactants, there exists a shallow layer of fluid moving predominantly downstream and away from the jet centreline. The lateral extent of this layer is far greater than that of the jet flow beneath it. This layer will be referred to as the surface current.

The evolution of the surface current with distance downstream may be seen from measurements of the mean flow field in planes at $x/d = 16$, 24, 32, 48, and 64. Contour plots of the streamwise mean velocity are shown in figure 7, and vector plots of the horizontal and vertical mean velocities are shown in figure 8. The surface current is barely visible at $x/d = 16$, but at $x/d = 24$ it is identifiable as a shallow

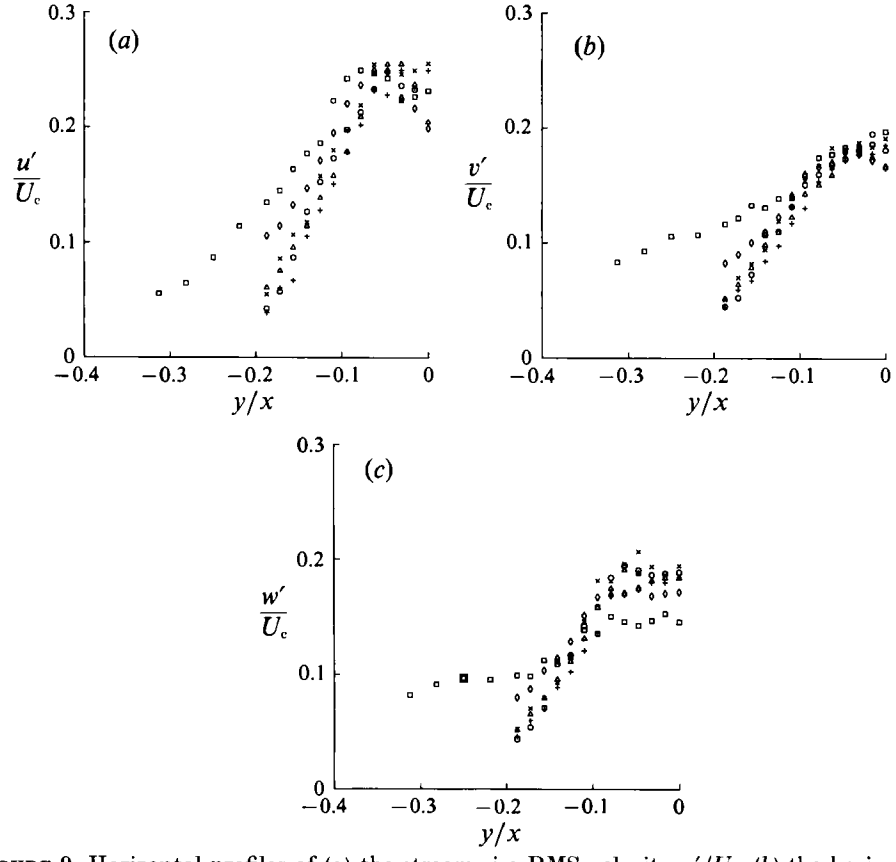

FIGURE 9. Horizontal profiles of (*a*) the streamwise RMS velocity u'/U_c, (*b*) the horizontal RMS velocity fluctuations v'/U_c and (*c*) the vertical RMS velocity fluctuations w'/U_c, at $x/d = 32$ for the shallow jet, $h/d = 2$. □, $z/d = 2$; ◇, $z/d = 1.5$; △, $z/d = 1$; ○, $z/d = 0$; ×, $z/d = -1$; +, $z/d = -2$.

layer just beneath the surface. At $x/d = 32$, the surface current is well established, extending laterally to beyond twice the width of the jet flow just beneath it, and its thickness has increased to about twice that at $x/d = 24$. At $x/d = 48$ and 64, the surface current is seen to be the dominant feature of the cross-stream flow.

Measurements of the turbulent velocity fluctuations and Reynolds stresses were obtained in planes parallel to the free surface. The RMS fluctuations are shown in figure 9, and the Reynolds stresses in figure 10. Near the surface, for $y/x = 0$, the magnitude of the vertical fluctuation w' is diminished well below those of the streamwise and cross-stream fluctuations u' and v', in agreement with the results of figure 4(*b*). However, within the surface current, for values of $y/x < -0.15$, the magnitudes of the horizontal and vertical fluctuations become almost equal, while that of the streamwise fluctuations continues to diminish. The Reynolds stress $\overline{uv}$, shown in figure 10(*a*), is seen to diminish toward zero within the current layer, indicating reduced turbulent mixing within the current. The remaining Reynolds stress components near the surface are very nearly zero, as is evident from figure 10(*b*, *c*). The results of the flow visualizations reported below show the current to contain fluid structures ejected from the jet. The observation that these structures remain relatively coherent indicates a reduced level of mixing within the current and is consistent with a low value of Reynolds stress measured within the current.

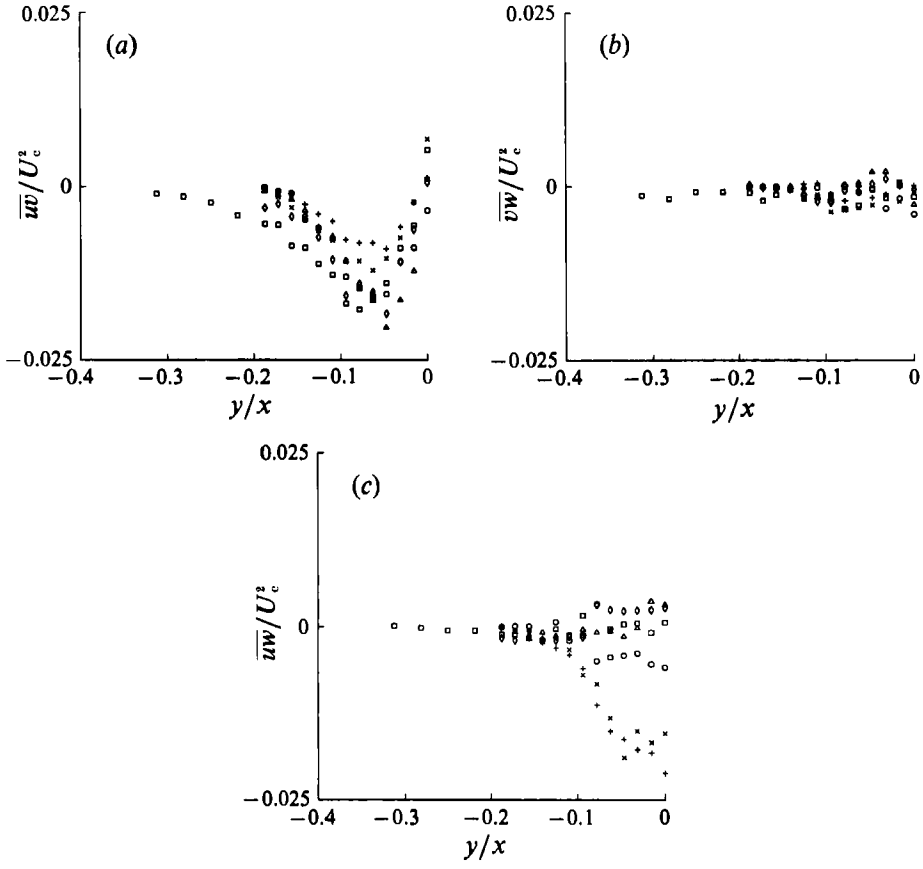

FIGURE 10. Horizontal profiles of the Reynolds stress: (*a*) $\overline{uv}/U_c^2$, (*b*) $\overline{vw}/U_c^2$, and (*c*) $\overline{uw}/U_c^2$, at $x/d = 32$ for the shallow jet, $h/d = 2$. □, $z/d = 2$; ◇, $z/d = 1.5$; △, $z/d = 1$; ○, $z/d = 0$; ×, $z/d = -1$; +, $z/d = -2$.

The Reynolds stress $\overline{uv}$ is negative in horizontal planes near the jet (figure 10*a*), and the velocity gradient $\partial U/\partial y$ is large and positive in these planes (figure 6*a*); the energy production term $-\overline{uv}(\partial U/\partial y)$ is therefore appreciable and positive in the region lying near and to either side of the jet. This term, and the previously discussed term $-\overline{uw}(\partial U/\partial z)$, which is positive above and below the jet, are the two dominant sources of turbulent energy production accompanying the transverse exchange of streamwise jet momentum.

The observed behaviour of the RMS velocity fluctuations in a region of small or vanishing Reynolds stress suggests that appreciable contributions to the velocity fluctuations may arise from unsteady, irrotational motions, such as from orbital motions in the flow beneath surface waves travelling perpendicular to the jet centreline. Such a motion contributes to the vertical and cross-stream fluctuations but not to the streamwise fluctuations. Observations of the wave field and the contribution to the RMS fluctuations from wave motions are discussed below.

The existence of a surface current does not obviously follow from considerations of a jet merging with its image above the surface, but the rapid lateral spreading has also been observed in the flow field of the three-dimensional wall jet. The measurements of Newman *et al.* (1972) and Launder & Rodi (1983) reveal that the wall jet exhibits a lateral spreading rate far greater than that found in free jets.

(a)

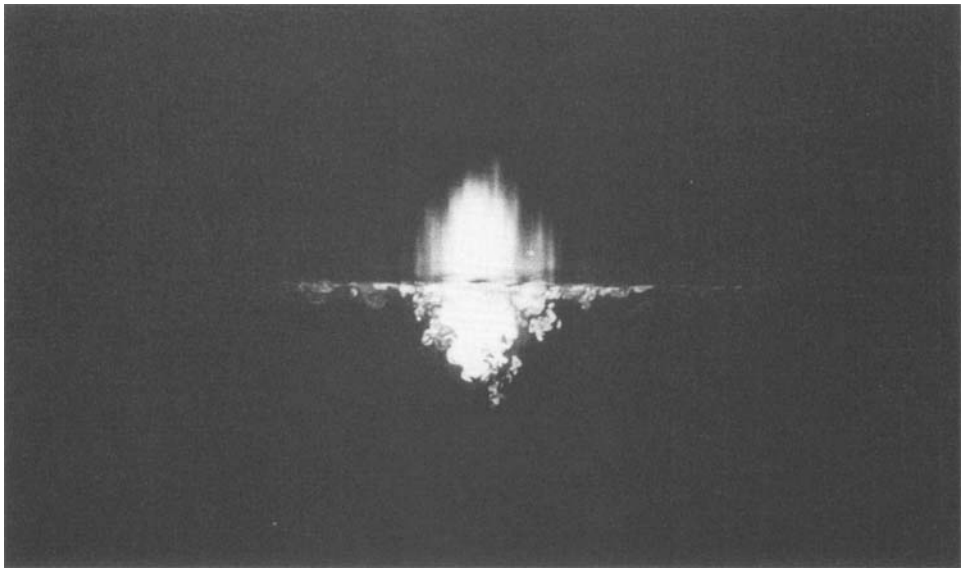

(b)

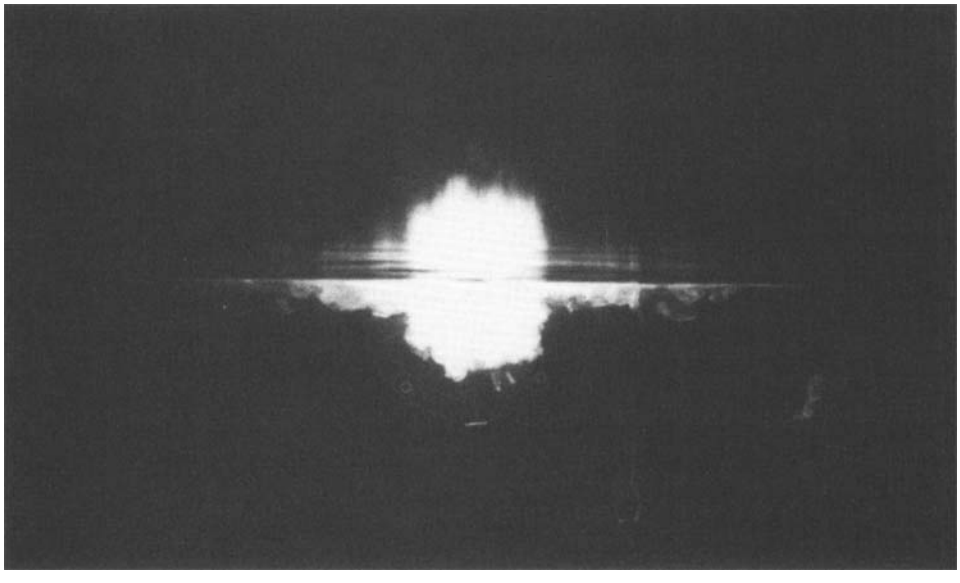

FIGURE 11. LIF photographs of the shallow jet, $h/d = 2$, issuing beneath a clean free surface. The laser light sheet was positioned in a vertical plane at $x/d = 32$. Exposure times are (a) 1/125 s and (b) 1/2 s.

Launder & Rodi (1983) attribute the higher lateral spreading rate to the creation of substantial streamwise vorticity, created either from a reorienting of vortex lines or through inhomogeneities in the Reynolds stress field. Liepmann (1990) reports that the near-field behaviour of the free-surface jet is governed by the formation of streamwise vorticity from instabilities in the transition region.

Bernal & Madnia (1988) made a comparison between the turbulent wall jet and the

turbulent free-surface jet and concluded that the two flows were fundamentally different, attributing this to the differing dynamics of vorticity at solid and free surfaces. However, their measurements did not reveal a surface current, for several possible reasons: measurements may not have been taken sufficiently close to the surface to resolve the shallow current, the lateral spreading of the jet may have been limited by the size of the facility, or surface contaminants may have inhibited the formation of the current.

The similarity between free-surface jets and wall jets is somewhat striking, suggesting that it is the presence of a boundary surface at which the normal velocity must vanish, rather than the no-shear or no-slip tangential condition that applies at that surface, that leads to the overall features observed in either flow, particularly to the strong lateral spreading rate. Differences in the spreading angle and the depth of the surface current or wall layer may arise from differences in the tangential boundary condition. Comparison of the iso-velocity contours of figure 7(*d*) for the free-surface jet (at $x/d = 48$, with $h/d = 2$ and $Re = 12700$) with those reported by Davis & Winarto (1980) for the wall jet (at $x/d = 48$, with $h/d = 2$ and $Re = 170000$) shows that the region of outward flow near the free surface is approximately one half the thickness of the region of outward flow near the solid wall. This is most likely a consequence of the different tangential boundary conditions: a free surface allows fluid motion in the plane of the surface, whereas at a solid surface, a boundary layer must form with a consequent displacement of the streamlines from the surface.

3.2. *Dye visualizations*

The interaction of the turbulent jet with the free surface was visualized using a laser-induced fluorescence technique. Fluorescein dye was added to fluid in the jet reservoir and the dyed fluid emanating from the jet was illuminated with a sheet of laser light. The light sheet was oriented either vertically to illuminate cross-stream planes or horizontally to illuminate planes parallel to the free surface.

With the light sheet oriented vertically and normal to the jet axis, the boundaries of the dyed fluid in the jet were observed to be spatially uneven and highly unsteady. Puffs of dyed fluid appeared to be emitted from the jet in random directions, and these puffs initially appeared to propagate outward, away from the jet. The puffs that were emitted downward into the entraining flow were rapidly slowed and were rarely observed to propagate far from the jet boundary. However, those puffs that were emitted near the clean free surface, having little downward velocity, were observed to continue to move parallel to the surface away from the jet boundary. These emissions propagated to several jet half-widths in a thin layer just below the surface. The average of many such emissions and their subsequent propagation outward gives rise to a mean outward flow of dyed fluid which is observed within the region of the surface current. Figure 11 shows a photograph in a cross-stream plane at $x/d = 32$ beneath a clean free surface, illustrating the ejected fluid that appears within the surface current.

Figure 12 shows a photograph in the same plane beneath a free surface initially contaminated with a uniform film of oleyl alcohol, an insoluble surfactant. The initial concentration was 1.3×10^{-7} cm^3 of surfactant per cm^2 of free surface, giving a mean surface pressure (or reduction in surface tension) of 9 dyn/cm. Fluid ejected from the jet did not spread as for a clean surface, and the surface current was not observed to form.

The effects of surface contamination on the trajectories of laminar vortex pairs were studied by Hirsa (1990). When the surface was clean, the vortices would

(*a*)

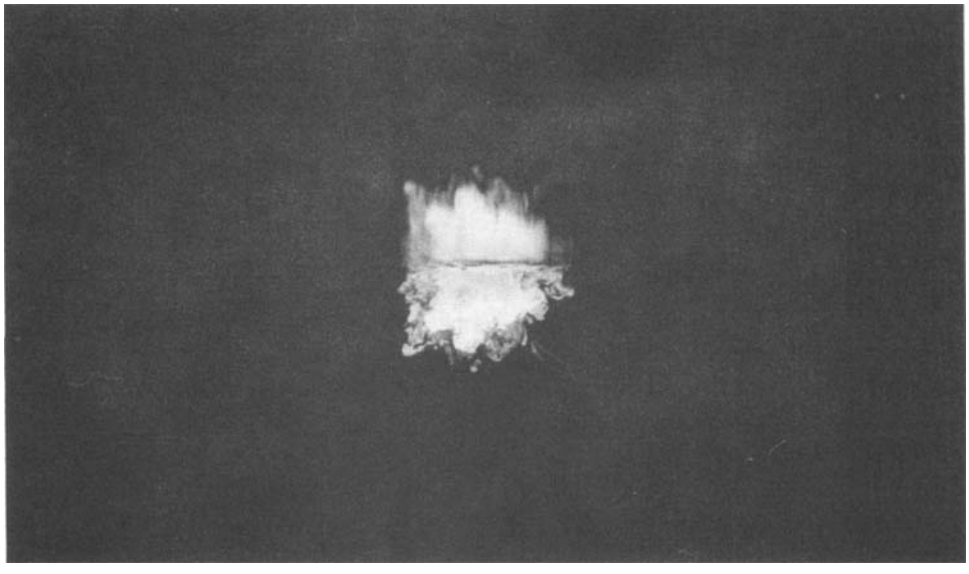

(*b*)

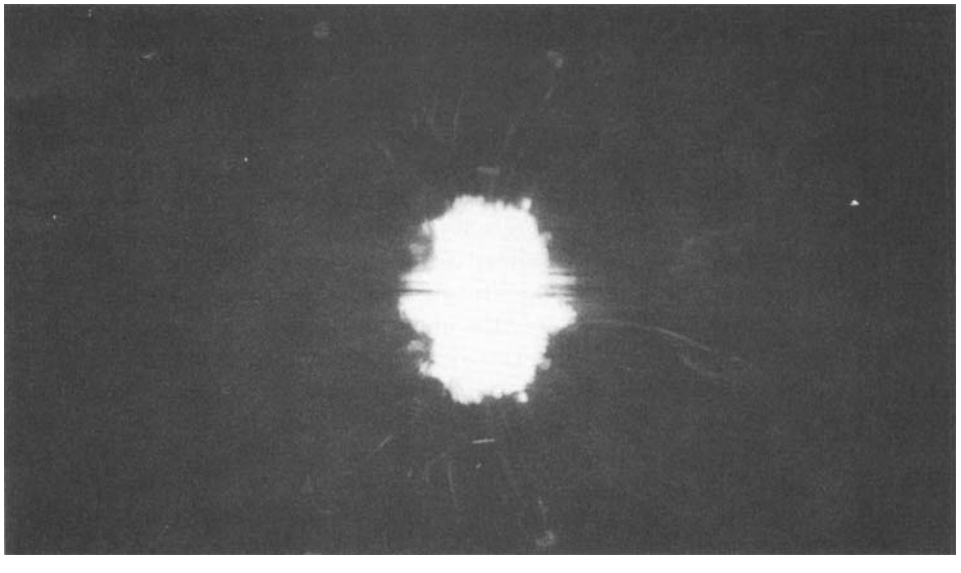

FIGURE 12. LIF photographs of the shallow jet, $h/d = 2$, issuing beneath a free surface contaminated with oleyl alcohol. The laser light sheet was positioned in a vertical plane at $x/d = 32$. Exposure times are (*a*) 1/125 s (top) and (*b*) 1/2 s.

propagate laterally beneath the surface in the manner of point vortices interacting with their images at a plan of symmetry. When the surface was contaminated, vorticity of opposite sign was generated beneath the contaminated surface outboard of each primary vortex as a result of the vortex interaction. This vorticity would interact with the primary vortices, rolling-up to form a pair of secondary vortices that then caused the primary vortices to turn downwards, or rebound, from the

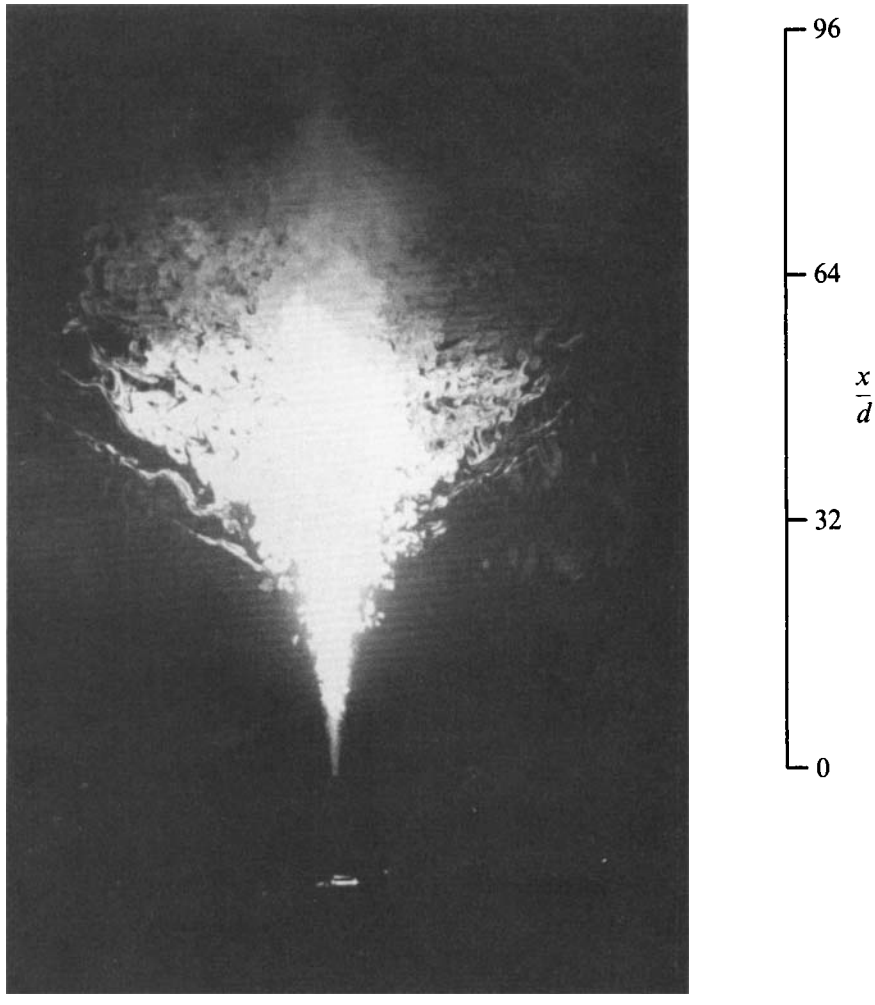

FIGURE 13. LIF photograph of the shallow jet, $h/d = 2$, issuing beneath a clean free surface. The laser light sheet was positioned in a horizontal plane approximately 0.3 cm below the free surface.

surface. It is suggested that a similar mechanism is effective in restricting the outward propagation of vortical structures, having substantial vorticity parallel to the surface, that are ejected from the jet beneath a contaminated free surface (Anthony *et al.* 1991).

The nature of the surface current beneath a clean free surface was investigated in planes parallel to the surface using a horizontal light sheet. Figure 13 shows an LIF visualization of the surface current made with the light sheet positioned just beneath the free surface. The boundaries of the dyed fluid spread initially at about 10° to the jet centreline, as is characteristic of the free jet. By 12 to 16 diameters downstream, the lateral spreading becomes much greater, with a half angle of spread of approximately 40°. The current layer shows strands or tendrils of dyed fluid that remain relatively coherent throughout the layer, and high concentrations of dye within the ejected fluid indicate that turbulent mixing is greatly diminished within the surface current. This reduced mixing is confirmed by the LDV measurements, which show the Reynolds stress $\overline{uv}$ to be diminished and the stresses $\overline{vw}$ and $\overline{uw}$ to be negligible within the surface current. Figure 14 shows an LIF visualization in a

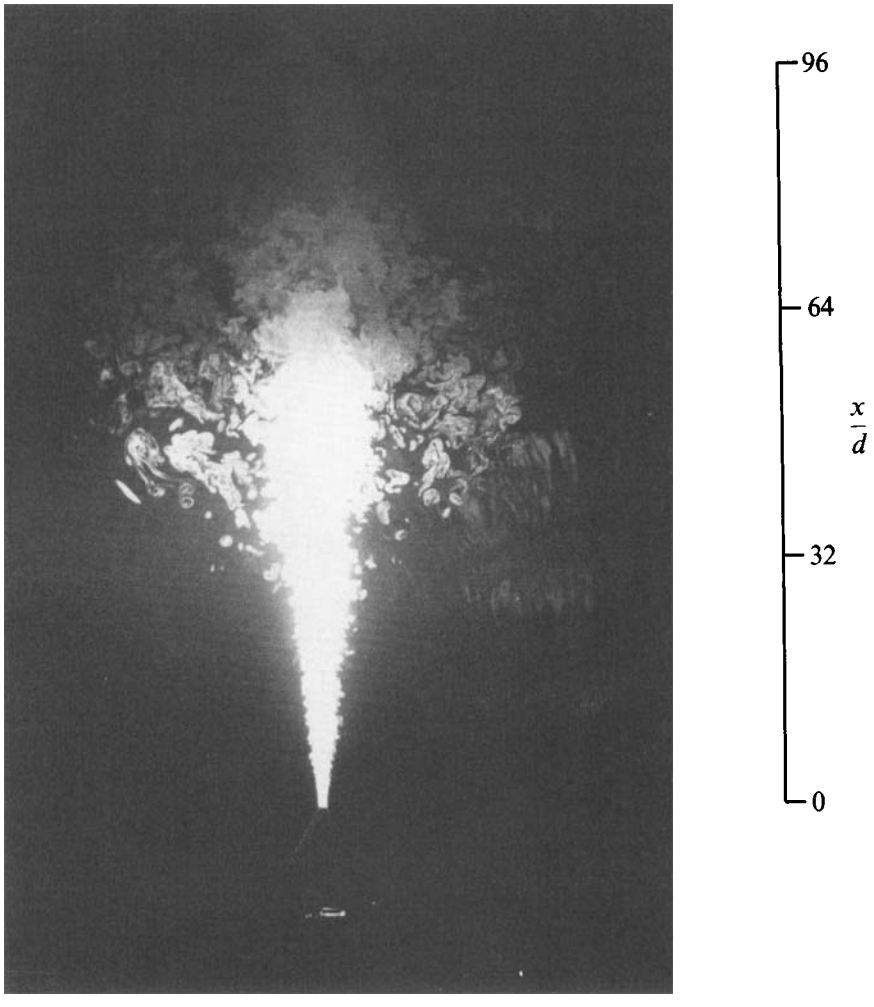

FIGURE 14. LIF photograph of the shallow jet, $h/d = 2$, issuing beneath a clean free surface. The laser light sheet was positioned in a horizontal plane through the jet centreline.

horizontal plane through the jet centreline. The small spreading angle characteristic of the free jet is apparent to about 24 diameters downstream, at which distance the surface current is revealed only by structures sufficiently large to intercept the light sheet from above. At this depth, the ejected structures no longer resemble strands, but appear instead as islands of dyed fluid.

The flow visualizations reported for the wall jet by Newman *et al.* (1972) and by Launder & Rodi (1983) were obtained by adding dye to the jet and viewing the jet both parallel and normal to the wall. The photographs of Newman *et al.* (1972) show the boundaries of the jet to spread at approximately 40° to the jet centreline, for a wall jet at Reynolds number $Re = 2800$ with the jet orifice attached to the wall ($h/d \approx 0.5$). Launder & Rodi (1983) showed the spreading angle to be sensitive to Reynolds number, reporting half-angles of spread up to 36° and attributing differences in the spreading of wall jets at the same Reynolds number to differing jet geometries at the exit plane.

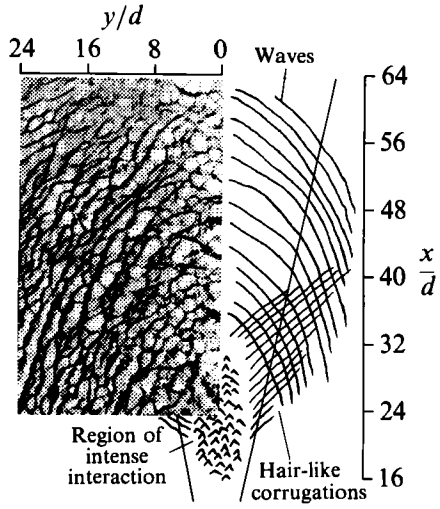

FIGURE 15. Shadowgraph and sketch showing surface deformations above the shallow jet, $h/d = 2$, beneath a clean free surface. Indicated in the sketch are closely spaced hair-like disturbances which were observed in the video images but were not resolved in the inset shadowgraph.

3.3. *Shadowgraph visualizations*

Figure 15 shows a shadowgraph image and sketch of the free-surface deformations. The left-hand side of the figure was obtained from a shadowgraph image digitally scanned into a personal computer and inverted black for white to show the crests of waves as dark rather than light. From video recordings of the shadowgraph images, these outward-travelling waves were determined to have wavelengths of approximately 1 to 4 cm and wave speeds of approximately 25 cm/s, very nearly the minimum wave speed for capillary–gravity waves on deep water. Comparison of the wave speed with the flow velocities measured by the LDV within the surface current shows the wave speed to be many times greater than the mean speeds within the current; essentially, the waves propagate on top of the surface current. The right-hand side of figure 15 shows a sketch of features visible on the video recordings but not discernable in the still photographs. Fine, hair-like corrugations of the wave fronts were observed to form between approximately $20 \leqslant x/d \leqslant 40$, on either side of the jet centreline. These hair-like corrugations are believed to be the result of waves propagating over the ejected structures observed in the LIF visualizations of the surface current.

The shadowgraph images of the free surface show considerable surface deformations near the jet centreline, where energetic structures within the jet interact with the free surface. Near the edges of this active region, the surface disturbances become identifiable as waves, travelling nearly perpendicular to the axis of the jet. These waves appear to arise from an accumulation or coalescence of the incoherent, small-scale surface disturbances that occur throughout the interaction region. Bernal & Madnia (1988) made measurements of the free-surface waves generated by the interaction of the jet with a free surface over a range of Reynolds number from $Re = 6300$ to 16000 and Froude number from $Fr = 1.2$ to 5.7. Their measurements showed that the waves generated in the interaction region propagate at large angles (40° to 60°) to the downstream direction, and the propagation angle is dependent on Reynolds number and jet depth.

The role of surface waves on the development of the surface jet flow is not clear.

The observed behaviour of the turbulence intensities within the surface current, with the magnitudes of the vertical and cross-stream fluctuations becoming almost equal and that of the streamwise fluctuations diminishing toward the current edges, is consistent with wave motions perpendicular to the jet centreline. The contributions to the RMS velocity fluctuations from orbital motions beneath surface waves were estimated from crude measurements of the wavelength and wave amplitude upon the current. These estimates yield values that are of the same order as the RMS velocity fluctuations measured with the LDV, indicating that much of the measured fluctuations can be attributed to the wave field, with the remaining fluctuations arising from turbulent motions within the fluid ejected from the jet.

4. Conclusions

Three-component LDV measurements of the mean velocity vector and Reynolds stress tensor were obtained in the turbulent flow field of a round jet issuing beneath and parallel to a free surface. The measurements reveal that near the jet centreline, where the interaction of jet flow with the free surface is most energetic, the RMS velocity fluctuations become anisotropic as the free surface is approached: the fluctuations normal to the surface are diminished, while those parallel to the surface are enhanced.

Characteristic of the jet interaction with the clean free surface was the formation of a shallow surface current, propagating downstream and laterally at an angle of approximately 40° to the jet centreline. LDV measurements of the mean velocity near the surface show that the width of this current is several times greater than the width of the primary jet flow beneath it, or the width of an axisymmetric free jet at the same downstream distance.

Flow visualization using fluorescent dye shows the surface current to contain fluid ejected from the jet. These ejections propagate outward to several jet half-widths in a thin layer just below the surface, and the average of many such ejections gives rise to a mean outward flow of dyed fluid. The ejected fluid is observed to form tendril-like structures aligned with the mean flow in the current. These structures remain coherent and contain relatively high concentrations of dye, indicating that turbulent mixing is greatly reduced within the surface current. This reduced mixing is confirmed by the LDV measurements, which show the Reynolds stress $\overline{uv}$ to be diminished and the stresses $\overline{vw}$ and $\overline{uw}$ to be negligible within the current.

The flow near the free surface resembles that found for a jet discharging parallel to a sold wall. In both cases, the spreading rate parallel to the wall is significantly greater than that normal to the wall. This similarity between the free-surface jet and the wall jet suggests that it is the presence of a plane (or nearly plane) boundary at which the normal velocity must tend to zero, rather than the conditions imposed on the tangential velocity or shear stress at the boundary, which leads to the formation of an outward flow parallel to the boundary. However, the thickness of the wall layer is at least twice that of the surface current. This is most likely a consequence of the differing tangential boundary conditions: a free surface allows fluid motion in the plane of the surface, whereas at a solid surface, a boundary layer must form along the wall.

The addition of an insoluble surfactant to the free surface was observed to suppress the formation of the surface current. We speculate that the physical mechanism acting to suppress the surface current is one similar to that found for vortex rings and pairs beneath contaminated free surfaces (see Bernal *et al.* 1989; Hirsa 1990).

Ejections of fluid from the jet, having appreciable vorticity parallel to the surface, cause secondary vorticity of opposite sign to be generated beneath the surfactant-covered surface. The interaction between ejected vorticity and this secondary vorticity inhibits the outward propagation of the ejected fluid and thereby suppresses the current. An initially uniform concentration of surfactant is redistributed by the flow from the jet, leading to a non-uniform (and unknown) concentration of surfactant, and hence of surface shear stress, in response to the flow beneath the surface. Further investigations of surfactant effects and determination of the surfactant concentration after the jet flow is established are necessary.

The interaction of the jet flow with the free surface leads to the generation of surface waves near the jet centreline. These waves, generated continually and apparently at random by large-scale structures in the jet flow, are observed to coalesce and to propagate in a direction nearly perpendicular to the jet axis. Under the conditions investigated, and with the free surface cleaned of surfactants, these waves were found to be capillary–gravity waves of wavelength 1–4 cm and wave speed approximately 25 cm/s.

Although the surface current arises from the ejection of turbulent fluid from the jet, the orbital motions beneath surface waves superposed on the current contribute significantly to the RMS velocity fluctuations near the surface. LDV measurements toward the edges of the surface current show that the cross-stream and vertical RMS velocity fluctuations are approximately equal and are greater than the streamwise fluctuations. In this region, the Reynolds stress $\overline{uv}$ is small, and the stresses $\overline{vw}$ and $\overline{uw}$ are negligible, indicative of reduced turbulent mixing within the surface current. This behaviour is distinctly different from that found near the jet centreline, where the velocity fluctuations normal to the free surface are diminished and the fluctuations parallel to the surface are enhanced. This difference is attributed largely to the wave motions superimposed upon the current.

Many of the flow phenomena observed here for a turbulent free-surface jet are found to occur in the wakes of surface ships. Johnston & Walker (1991) have recently investigated the flow field in the wake of a ship model. Their observations, from dye visualizations and shadowgraph images of the free surface, show a turbulent surface layer which spreads more rapidly when the ship model is self-propelled. They observe a turbulent region in the near wake in which small-scale surface disturbances are created. At the edges of this turbulent region, these disturbances coalesce into relatively organized waves which are independent of the Kelvin wave pattern and propagate outward into the irrotational free stream.

Quantitative measurements of the velocity field and surface deformations in the wakes of surface ships, as well as investigations of the influence of other factors, such as surfactants, ambient waves and currents, and breaking waves and bubble entrainment, on the nature and persistence of the wake signature are necessary to obtain a better understanding of this complicated problem.

The authors wish to acknowledge the support of the Office of Naval Research University Research Initiative Program for Ship Hydrodynamics at the University of Michigan, contract number N000184-86K-0684, and of the ONR-sponsored Surface Ship Wake Program at the David Taylor Research Center. We are also grateful to Amir Hirsa for his assistance in obtaining the flow visualizations.

REFERENCES

ABRAMOVICH, G. N. 1963 *The Theory of Turbulent Jets.* MIT.

ANTHONY, D. G. 1990 The influence of a free surface on the development of turbulence in a submerged jet. Ph.D. thesis, University of Michigan.

ANTHONY, D. G., HIRSA, A. & WILLMARTH, W. W. 1991 On the interaction of a submerged turbulent jet with a clean or contaminated free surface. *Phys. Fluids* A **3**, 245–247.

BERNAL, L. P., HIRSA, A., KWON, J. T. & WILLMARTH, W. W. 1989 On the interaction of vortex rings and pairs with a free surface for varying amounts of surface active agent. *Phys. Fluids* A **1**, 2001–2004.

BERNAL, L. P. & MADNIA, K. 1988 Interaction of a turbulent round jet with the free surface. *Proc. 17th Symp. Naval Hydrodynamics.* Washington: National Academy Press.

DAVIS, M. R. & WINARTO, H. 1980 Jet diffusion from a circular nozzle above a solid wall. *J. Fluid Mech.* **101**, 201–221.

GAINES, G. L. 1966 *Insoluble Monolayers at Liquid-Gas Interfaces.* Interscience.

HIRSA, A. 1990 An experimental investigation of vortex pair interaction with a clean or contaminated free surface. Ph.D. thesis, University of Michigan.

JOHNSTON, V. G. & WALKER, D. T. 1991 Experimentally observed features of the turbulent near-wake of a model ship. *Tech. Rept.* 92–1, Univ. Mich. Program in Ship Hydrodynamics, ONR Contract N000184-86-K-0684, Jan. 1992.

KOMORI, S., UEDA, H., OGINO, F. & MIZUSHIMA, T. 1982 Turbulence structure and transport mechanism at the free surface in an open channel flow. *Intl J. Heat Mass Transfer* **25**, 513–521.

LAUNDER, B. E. & RODI, W. 1981 The turbulent wall jet. *Prog. Aerosp. Sci.* **19**, 81–128.

LAUNDER, B. E. & RODI, W. 1983 The turbulent wall jet – measurements and modeling. *Ann. Rev. Fluid Mech.*, **15**, 429–459.

LIEPMANN, D. 1990 The near-field dynamics and entrainment field of submerged and near-surface jets. Ph.D. thesis, University of California, San Diego.

LYDEN, J D., HAMMOND, R. R. LYZENGA, D. R. & SHUCHMAN, R. A. 1988 synthetic aperture radar imaging of surface ship wakes. *J. Geophysical Res.* **93** (C10), 12293–12303.

MCLAUGHLIN, D. K. & TIEDERMAN, W. G. 1973 Biasing correction for individual realization of laser anemometer measurements in turbulent flow. *Phys. Fluids* **16**, 2082–2088.

MUNK, W. H., SCULLY-POWER, P. & ZACHARIESEN, F. 1987 Ship wakes from space: the Bakerian lecture, 1986. *Proc. R. Soc. Lond.* A **412**, 231–254.

NEWMAN, B. G., PATEL, R. P., SAVAGE, S. B. & TJIO, H. K. 1972 Three-dimensional wall jet originating from a circular orifice. *Aeronaut. Q.* **23**, 188–200.

RAJARATNAM, N. 1976 Turbulent Jets. Elsevier.

RAJARATNAM, N. & HUMPHRIES, L. A. 1984 Turbulent non-buoyant surfaces jets. *J. Hydraul. Res.* **22**, 103–115.

RAJARATNAM, N. & HUMPHRIES, L. A. 1984 Turbulent non-buoyant surface jets. *J. Hydraul. Res.* **22**, 103–115.

RAJARATNAM, N. & SUBRAMANYAN, S. 1985 Plane turbulent buoyant surface jets. *J. Hydraul. Res.* **23**, 131–146.

RASHIDI, M. & BANERJEE, S. 1988 Turbulence structure in free-surface channel flows. *Phys. Fluids* **31**, 2491–2503.

SWEAN, T. F., RAMBERG, S. E., PLESNIAK, M. W. & STEWART, M. B. 1989 Turbulent surface jet in channel of limited depth. *J. Hydraul. Engng.* **115**, 1587–1606.

WILLMARTH, W. W. 1987 Design of three component fiber optic laser Doppler anemometer for wake measurements in a towing tank. *Proc. Intl Towing Tank Conf., 18–24 Oct. 1987, Kobe, Japan*, Vol. 2, pp. 338–391.

WYGNANSKI, I. & FIEDLER, H. 1969 Some measurements in the self-preserving jet. *J. Fluid Mech.* **38**, 577–612.